Beta-amyloid oligomerisation monitored by intrinsic tyrosine fluorescence

ARTICLE *in* PHYSICAL CHEMISTRY CHEMICAL PHYSICS · MARCH 2011

Impact Factor: 4.49 · DOI: 10.1039/c0cp02652b · Source: PubMed

3 AUTHORS, INCLUDING:

Mariana Amaro

Academy of Sciences of the Czech Republic

18 PUBLICATIONS **84** CITATIONS

SEE PROFILE

PCCP

Cite this: *Phys. Chem. Chem. Phys.*, 2011, **13**, 6434–6441

www.rsc.org/pccp

PAPER

Beta-amyloid oligomerisation monitored by intrinsic tyrosine fluorescence

Mariana Amaro, David J. S. Birch and Olaf J. Rolinski*

Received 24th November 2010, Accepted 26th January 2011
DOI: 10.1039/c0cp02652b

Aggregation of the peptide beta-amyloid is known to be associated with Alzheimer's disease. According to recent findings the most neurotoxic aggregates are the oligomers formed in the initial stages of the aggregation process. Here we use beta-amyloid's (Aβ's) intrinsic fluorophore tyrosine to probe the earliest peptide-to-peptide stages of aggregation, a region often merely labelled as a time lag, because negligible changes are observed by the commonly used probe ThT. Using spectrally resolved fluorescence decay time techniques and analysis we demonstrate how the distribution of 3 rotamer conformations of the single tyrosine in Aβ tracks the aggregation across the time lag and beyond according to the initial peptide concentration. At low Aβ concentrations (≤ 5 μM), negligible aggregation is observed and this is mirrored by little change in the fluorescence decay parameters, providing a useful baseline for comparison. At higher concentrations (≈ 50 μM), and contrary to what is generally accepted from ThT studies the rate of aggregation can be described by an exponential growth to a plateau in terms of the relative contributions of two of the three rotamers, with a characteristic aggregation time of ≈ 33 h.

Introduction

Some misfolded proteins have a tendency to aggregate, causing depositions of protein oligomers and fibrils (amyloids),[1] which may lead to the disease of amyloidosis. When amyloid deposition occurs in the brain it causes neurodegeneration. Alzheimer's disease is one such example of amyloidosis and the most common type of neurodegenerative disease.

The mechanism explaining how amyloidoses cause cell death in neurodegenerative diseases still evades our knowledge. Plaques of aggregated amyloid fibrils, originally suggested as the cause of the disease are no longer considered to be the pathogenic factor. Instead, the small soluble oligomers[2,3] formed at the beginning of the aggregation process are now believed to be the main cytotoxic entities. It is therefore important to fully understand the very early stages of amyloid aggregation as it can help in the design of more effective therapeutics not only for the Alzheimer's but for all amyloidoses. Alzheimer's is associated with aggregation of the beta-amyloid (Aβ) peptide. Aβ peptide is a cleavage product of the β-amyloid precursor protein (APP) and is 40 or 42 amino acids (a.a.) long and contains only one tyrosine (Tyr) aminoacid in position 10. Aβ can be found in the plasma and cerebrospinal fluid of healthy humans and other mammals, and the 40 a.a. long form [Aβ(1–40)] is most common.[4] Amyloid fibril formation appears to be a multistep process during which a number of intermediate aggregates are formed. The aggregation starts with the coalescence of peptide monomers to form small oligomeric aggregates such as dimers, trimers, *etc*. These small oligomers then grow further in size and complexity evolving into protofibrils and then mature amyloid fibrils. The full mechanism of amyloid aggregation is still unclear. Finding a detailed description is a challenge because of the difficulty monitoring changes experimentally *in situ* and in identifying the nanometre scale process of aggregation at its early stages due to the nanoscale transient species involved.[5–7]

In this paper we explore the sensitivity of fluorescent molecules to the interactions between them and their surroundings within an Angström (Å) to nanometre scale, making use of the proven capabilities of fluorescence techniques in the study of structure and dynamics of microheterogeneous systems. Hitherto a number of fluorescence techniques have been applied to monitor different stages of amyloid aggregation. The most popular approach is based on Thioflavin T (ThT), which binds to beta-sheets in amyloid fibrils and stabilises the ThT planar (fluorescent) form leading to an increased quantum yield. Increase in ThT fluorescence reports on the appearance of beta-sheets during amyloid fibril assembly and growth.[8–10] Other techniques such as fluorescence anisotropy,[11] Förster resonance energy transfer[12] and cross correlation spectroscopy,[13] have also been used for monitoring prefibrillar aggregates. An essential drawback of these techniques is that they are only sensitive at the later stages of aggregation when aggregates of several or more peptides are already formed. Moreover, they have another disadvantage in their use of extrinsic fluorophores having the potential to perturb both the native structure and the aggregation kinetics.

Photophysics group, Centre for Molecular Nanometrology, Department of Physics, Scottish Universities Physics Alliance, University of Strathclyde, 107 Rottenrow, Glasgow G4 0NG, UK. E-mail: o.j.rolinski@strath.ac.uk

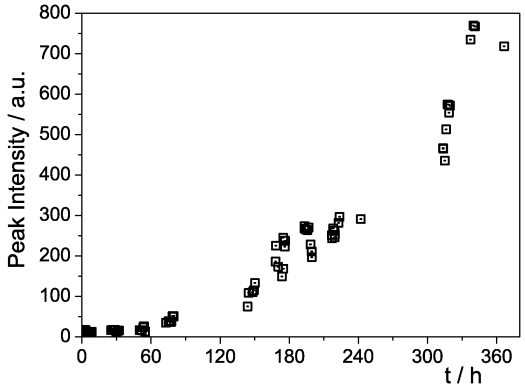

Fig. 1 Fluorescence emission spectral peak intensity of ThT at different stages of Aβ aggregation. The size of each point on the plot represents the experimental error (3 standard deviations).

Fig. 1 shows our measurements with ThT[14] agree with what has been reported previously[15] in terms of aggregation kinetics characterised by a time lag and growth function given by

$$F(t) = A + \frac{B}{1 + \exp[-(t - t_0)/\tau_a]} \qquad (1)$$

where A and B are experimental parameters relevant to the concentrations of fibrils, and t_0 and τ_a are the lag time and fibril growth time, respectively.

In this paper we show how the alternative approach based on Aβ's intrinsic fluorescence of Tyr eliminates the drawbacks of extrinsic fluorophore-based methods and can be used to monitor oligomer formation non-invasively starting from the very early onset of single peptide-to-peptide interactions. We have already demonstrated the sensitivity of Tyr lifetime measurements to aggregation at the stages much earlier than widely reported ThT steady-state measurements[14] but here we take the approach further by a more detailed investigation of the role of the initial monomer peptide concentration and combine the lifetime and spectral data to better understand the underlying photophysics.

The complexity of Tyr fluorescence decay, also observed in our previous research,[14] is often explained using a rotamer model. The peptide bonds of the a.a. chain are relatively rigid, but rotations are possible around single bonds. The C_α–C_β chemical bond in Tyr residue can rotate (Fig. 2) giving rise to the possibility of different conformations called rotamers. According to the Tyr rotamer model[16] rotation tends to cluster

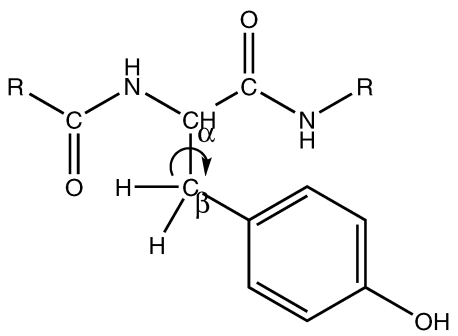

Fig. 2 Structure of tyrosine residue showing the possible rotation around C_α–C_β bond.

around three defined angles $\gamma^1 = 180°, +60°, -60°$. The phenol group therefore can change between three well defined potential wells. In each rotameric conformation the phenol group is exposed to different environments and remains at different distances from potential quenching groups within the peptide chain. As the fluorescence decay is determined by the local interactions between the phenol ring and its micro-environment each of the excited state rotamers has its own decay, usually characterised by its specific lifetime.

Any change in the fluorophore's surroundings (in the Å scale) is expected to modify the fluorescence decay, thus the aggregation of single Aβ peptides is thought to cause changes in Tyr fluorescence response. Hence we have used Tyr lifetime responses as fingerprints of different stages of initial Aβ misfolding and aggregation leading to the formation of oligomers. Using this approach, we have investigated how the initial monomer concentration affects Aβ aggregation and monitored this aggregation over the period of several days.

Materials and methods

Aβ(1–40), hexafluoroisopropanol (HFIP), *N*-(2-hydroxyethyl)-piperazine-*N*′-(2-ethanesulfonic acid) buffer solution (HEPES) were purchased from Sigma-Aldrich (Poole, UK). To monitor the early stages of aggregation it was crucial to start from a monomeric solution of peptides as the presence of preformed aggregates would influence the kinetics of the process. A monomer solution was achieved by treating the received Aβ(1–40) with HFIP.[17] Treatment consisted of dissolving the Aβ powder in pure HFIP to a concentration of 10^{-4} M and sonicating for at least 10 min. The peptide containing solution was then aliquoted into Eppendorf® LoBind microcentrifuge tubes and the alcohol allowed to evaporate. For thorough HFIP removal the resulting peptide films were dried under vacuum. The aliquots were then stored at −20 °C. To prepare a sample an aliquot was taken and allowed to thermally stabilize at room temperature prior to opening. The peptide film was then re-suspended in HEPES buffer (100 mM; pH: 7.3) and sonicated for about 2 min at 37 °C. The samples were prepared directly before the first measurement; all cuvettes and buffer solutions were in thermal equilibrium at the desired temperature before use.

A Perkin-Elmer LS-50 B luminescence spectrometer was used for fluorescence spectral measurements. Tyr was excited at 279 nm and its fluorescence was collected in the range 300–360 nm. Fluorescence decays were recorded using the time-correlated single-photon counting (TCSPC) technique on an IBH Fluorocube fluorescence lifetime system (Horiba Jobin Yvon IBH Ltd., Glasgow, UK) equipped with both excitation and emission monochromators. An AlGaN version of a pulsed light emitting diode was used in this work at 279 nm in order to excite Tyr directly.[18] The optical pulse duration was ~600 ps (fwhm) and repetition rate 1 MHz. Measurements were performed at controlled temperature using a temperature-controlled sample holder connected to a Neslab RTE-11 thermostat (Thermo Scientific UK).

The complex nature of protein aggregation makes the time between sample preparation and the experiment, T, and the wavelength at which the decay is measured, λ, critical factors

in determining the fluorescence decay. This implies the fluorescence decay being a parametrical function of T and λ, *i.e.* $I(t;T,\lambda)$. Therefore two types of lifetime experiments were performed in this research. To monitor the influence of the peptide aggregation on Tyr fluorescence decay, the decays $I_\lambda(t;T)$ were measured with $\lambda = 315$ nm at increasing times T after sample preparation. In order to obtain the wavelength-dependent decays of Tyr, the decays $I_T(t;\lambda)$ at fixed times T were collected for different emission wavelengths λ between 300 and 330 nm with wavelengths steps of 3 nm.

The DAS6 (IBH) data analysis package was used for 1- to 3-exponential deconvolution analyses using a non-linear least squares method. A three exponential decay model (2) was chosen to fit the data

$$I(t;T,\lambda) = \sum_{i=1}^{3} \alpha_i \exp[-t/\tau_i] \qquad (2)$$

on the basis of the best-fit χ^2 values and random distributions of weighted residuals obtained for a 3-exponential function when applied to all the decays. An index i refers to one of three rotamers and the pre-exponential components α_i and corresponding lifetimes τ_i are regarded as functions of T and λ. Fitting the data to one and two-exponential models recovered statistically unacceptable results.

The fractional contributions of each lifetime component f_i were calculated as

$$f_i = \frac{\alpha_i \tau_i}{\sum_{k=1}^{3} \alpha_k \tau_k} \qquad (3)$$

Fluorescence decays measured for the different emission wavelengths λ allowed determination of the wavelength dependent fractional contributions $f_i(\lambda)$. The decay associated spectra (DAS) $F_i(\lambda)$, each presenting a fluorescence spectrum of the relevant rotamer Y_i, were calculated from the fractional contributions $f_i(\lambda)$ according to

$$F_i(\lambda) = F(\lambda) f_i(\lambda) \qquad (4)$$

where $F(\lambda)$ is the overall steady-state fluorescence spectrum.

Results and discussion

The simplistic rotamer model, considered in this paper, implies a three-exponential fluorescence decay of Tyr with the recovered lifetimes reporting on the excited-state kinetics of individual rotamers. In this section we demonstrate, that all decays of Tyr detected exhibit a three-exponential character by means of the χ^2 goodness of fit and the distribution of residuals criteria.

However, in order to fully confirm the suitability of the rotamer model to interpret lifetime data, the recovered parameters are expected to reflect fluorescence processes, which are molecular distance-dependent (like fluorescence quenching, proton/electron transfer, fluorescence resonance energy transfer, *etc.*), and thus are likely to accompany peptide aggregation.

Alternatively, if the recovered parameters are not consistent with the basic kinetics, the extension of the simple model is considered.

Effect of initial monomer concentration

To investigate Tyr's performance as an intrinsic reporter of aggregation present naturally in the Aβ peptide we measured its fluorescence decay at different peptide concentrations. As the fluorescence decay can be affected by the mutual interactions between Aβ peptides, the monomer concentration in solution might influence the complex fluorescence response of Tyr.

The lifetime measurements were performed at 37 °C for 8 samples of increasing Aβ concentrations, namely 5, 12, 20, 27, 35, 42, 50 and 57 μM. For comparison, in our previous report[14] only one peptide concentration of 30 μM was investigated. Our intention was to collect fluorescence decays prior to aggregation. However, it cannot be excluded that the aggregation in at least some of the samples has started immediately after sample preparation, before or indeed progressed during the measurement. In order to maintain the same experimental conditions in all the samples, the lifetime measurement of each sample was started exactly ten minutes after its preparation.

The retrieved lifetimes (τ_i) and fractional contributions (f_i) as function of Aβ concentration are shown in Fig. 3a and b, respectively. The lifetime values (Fig. 3a) do not change markedly with concentration of Aβ peptide, but the fractional contributions of decay lifetimes (Fig. 3b) depend on the

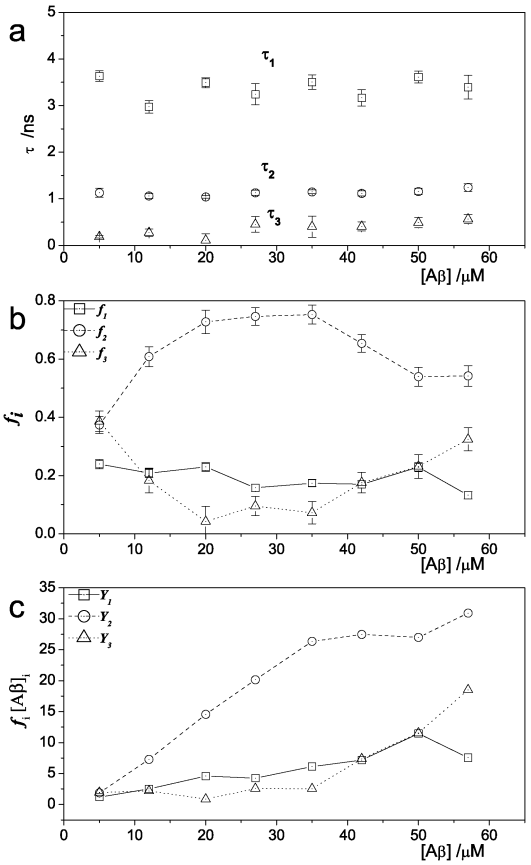

Fig. 3 Parameters obtained from fitting Tyr fluorescence decay to a 3 exponential decay model. (a) Tyr fluorescence decay time; (b) fluorescence intensity fractional contributions; (c) population of tyrosine rotamers Y_1, Y_2, Y_3, as functions of initial Aβ monomer concentration. Experimental errors are 3 standard deviations.

peptide concentration quite significantly. The fractional contribution f_1 (associated to a rotamer hereinafter referred as Y_1 with the characteristic lifetime $\sim$3.4 ns) remains constant, while the dependencies of f_2 (Y_2, $\sim$1.1 ns) and f_3 (Y_3, $\sim$0.4 ns) on concentration are non-monotonic. Up to the Aβ concentration of $\sim$30 μM there is an increase in fractional contribution f_2 and decrease in f_3, while for the higher Aβ concentrations, these trends reverse. The effect of Aβ concentration on rotamers contributions to total fluorescence becomes more clear on the plot in Fig. 3c, where the values of f_i[Aβ] (proportional to fluorescence intensities of the rotamers Y_i), are plotted as the function of [Aβ]. The curves in the plot on Fig. 3c represent the intensities of fluorescence of each rotamer. Their changes with [Aβ] can be interpreted in terms of the changes in the relevant rotamers populations, providing their quantum yields remain unaffected by the concentration of the peptide. Constant values of quantum yields cannot be confirmed definitely, but are supported by stable values of lifetimes measured for different peptide concentrations.

Accepting the stability of quantum yields leads to the conclusion that increasing the concentration of the peptide means, up to the concentration of about 30 μM, a proportional increase of the populations of three rotamers, with dominating rotamer Y_2. For higher concentrations Y_2 growth stops and the population of rotamer Y_3 starts to increase. Rotamer Y_1 growths linearly with [Aβ], which may be an indication of Y_1 being less sensitive to the environment.

The fact that Aβ's Tyr shows a high sensitivity to the presence of neighbouring Aβ monomers indicates that Tyr can be used as a non-invasive intrinsic sensor to study the Aβ peptide and its process of aggregation into amyloid fibrils.

Evolution of fluorescence response with peptide aggregation

As it is expected that the aggregation process depends on the initial concentration of peptides, we investigated simultaneously two samples of different initial monomer concentrations and their lifetime responses $I(t;T,315\text{ nm})$ were followed over the course of about 2 weeks. The first sample was of a low concentration of initial Aβ monomers, 5 μM, and the second was of 50 μM.

(i) Low concentration sample. The retrieved lifetimes (τ_i) and fractional contributions (f_i) as the functions of aggregation time for the low concentration sample (LC) are shown in Fig. 4a and b, respectively. It can be seen that the lifetime values are stable during the course of the 210 h of the experiment. The fractional contributions of the decay lifetimes (Fig. 4b) show some, but not large, change throughout the experiment. No significant change in all the parameters suggests the LC is fairly stable and aggregation does not occur or occurs at a slow rate and is unnoticeable during the first 210 h. This is confirmed by the ratio of f_1 to f_2 values, which can be used as an indicator of aggregation.[14] It can be seen (Fig. 4c) that no significant changes in f_1/f_2 occur, with its value around the level of 0.864 ± 0.018.

To better understand the kinetics of Tyr in the LC sample, its fluorescence decays were then detected at the different emission wavelengths. The sample can be considered as stable, as no further evolution in Tyr decay was observed at $T > 210$ h.

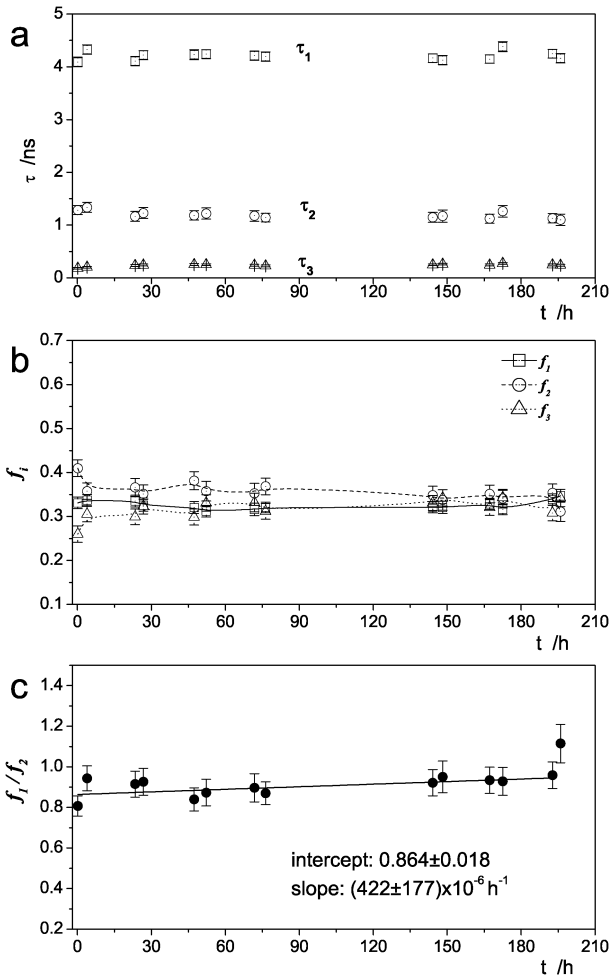

Fig. 4 Parameters obtained from fitting Tyr decay in the LC sample to a 3 exponential decay model. (a) Tyr fluorescence decay time; (b) fluorescence intensity fractional contributions; (c) ratio between decay times fractional contributions f_1/f_2; data fitted to a linear regression.

The parameters obtained from fitting to a 3 exponential decay model are shown in Fig. 5a (lifetimes) and b (fractional contributions).

Fig. 5a shows a small but clear increase in the recovered lifetimes with the detection wavelength. This effect cannot be explained in terms of a simple three-rotamer model, each being represented by a fixed fluorescence lifetime. Perhaps the observed changes in lifetimes indicate that the rate of solvation of Tyr's phenol group following electronic excitation is comparable to the rate of fluorescence, thus lifetimes detected at longer λ are longer. It is worth noting that the relative changes in these three lifetimes, *i.e.* $(\tau_i(324\text{ nm}) - \tau_i(300\text{ nm}))/\tau_i(300\text{ nm}))$ are 0.26, 0.80 and 1.91 ns for Y_1, Y_2 and Y_3, respectively. This suggests the relaxation times of the phenol groups in all three rotamers are long (nanoseconds instead of typical picoseconds) but are different for each rotamer due to different local surroundings. Alternatively, the observed changes in fluorescence lifetimes are caused by the actual kinetics being more complex than a 3-exponential model considered in this paper.

The lifetime results (Fig. 5a and b) were used with the steady-state emission spectrum of the sample to create the DAS $F_i(\lambda)$ (Fig. 5c) representing the separate spectra of three rotamers

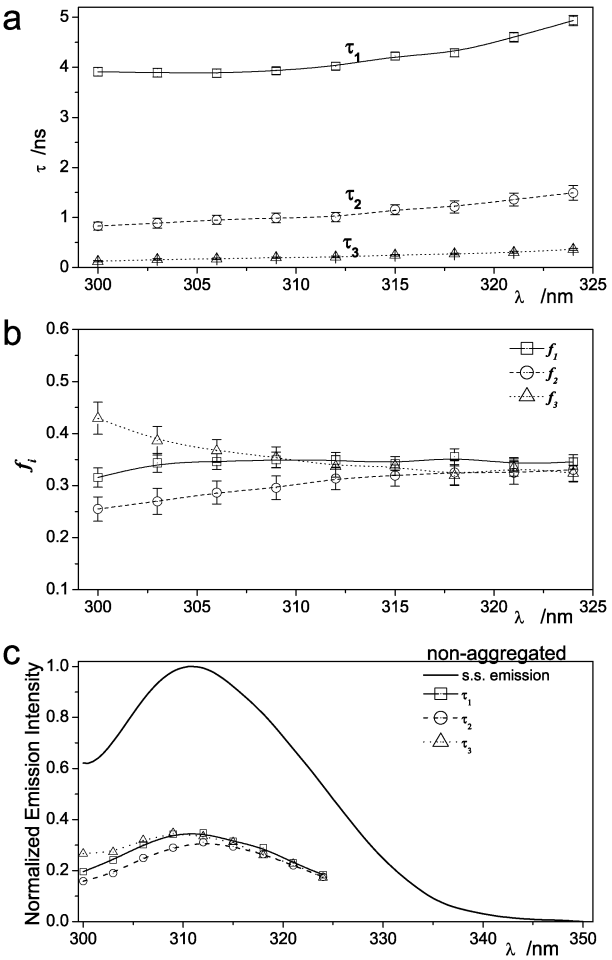

Fig. 5 Parameters obtained from fitting Tyr decay in the LC sample. (a) fluorescence decay times obtained from fitting Tyr decay to a 3 exponential decay model as function of wavelength; (b) fluorescence intensity fractional contributions; (c) full line: emission spectra of Aβ's Tyr; dotted lines: Decay Associated Spectra for the three retrieved decay times; All experimental errors are 3 standard deviations.

Y_1, Y_2 and Y_3. One can observe that the individual spectra are almost identical indicating that all forms contribute a similar profile and intensity to the overall fluorescence. The relatively large differences in f_i values at short wavelengths (300–305 nm) (see Fig. 5b) affect the DAS of Y_1 and Y_2 to a small extent. The fact that the DAS of shorter-lived rotamer Y_3 is slightly higher can be rationalized by the possibility of scattered light affecting the measurements at such low wavelengths. Due to the virtual null lifetime of scattered light its effects are more noticeable in the shorter lifetime components of the decay. If all rotamers exhibit the same quantum yields, the result in Fig. 5c would imply equal abundance of the three rotamers in the sample. However, due to substantially different lifetimes shown by the rotamers, different quantum yields seems to be more likely. Indeed, if we assume that the rate of the radiative transition for Tyr is $k_0 = 1/\tau_0$ and the rate of non-radiative transition (*e.g.* due to quenching mechanism) of the rotamer Y_i is k_i, the resulting lifetime τ_i of the Y_i form is given by

$$\frac{1}{\tau_i} = \frac{1}{\tau_0} + k_i \tag{5}$$

and its quantum yield η_i is

$$\eta_i = \frac{k_0}{k_0 + k_i} = \frac{\frac{1}{\tau_0}}{\frac{1}{\tau_0} + k_i} = \frac{\tau_i}{\tau_0} \tag{6}$$

As τ_0 is unknown, we cannot estimate quantum yields of the rotamers, but their concentrations $[Y_i]$ can be worked out. The total fluorescence emitted by the rotamer Y_i, namely $\int F_i(\lambda)\mathrm{d}\lambda$, is proportional to the rotamer concentration $[Y_i]$ and its quantum yield η_i. Thus

$$\int F_i(\lambda)\mathrm{d}\lambda = \beta\eta_i[Y_i] \tag{7}$$

where β is the coefficient of proportionality. From (7) and (6)

$$[Y_i] = \frac{\tau_0}{\beta}\frac{\int F_i(\lambda)\mathrm{d}\lambda}{\tau_i} \tag{8}$$

As $[Y] = \sum_i [Y_i]$, we can finally write

$$[Y_i] = [Y]\frac{\tau_i^{-1}\int F_i(\lambda)\mathrm{d}\lambda}{\sum_{j=1}^{3}\tau_j^{-1}\int F_j(\lambda)\mathrm{d}\lambda} \tag{9}$$

As the total concentration $[Y]$ is known (5 μM), we can use eqn (9) to estimate the concentrations of individual rotamers. For the LC sample, they are 0.22 μM (4.45%), 0.75 μM (15.10%) and 4.02 μM (80.45%), for Y_1, Y_2, and Y_3, respectively. The percentage contributions shown here represent the occurrence of Tyr rotamers in a solution of Aβ monomers.

(ii) High concentration sample. The lifetimes and fractional contributions obtained for the HC (50 μM) sample are shown in Fig. 6a and b, respectively. The lifetimes show a very slow increase with time T, while the changes in the fractional contributions are quite significant. Contrary to the LC sample, all three f_i factors change with time, which may indicate a new process, not observed in LC, likely the effect of the spontaneous aggregation of the Aβ peptides. Note that the initial f_i values are very close to the result obtained for 50 μM Aβ in the initial monomer concentration experiment with dominating f_2 contribution. For the later times T (Fig. 6b), f_2 decreases which is accompanied by increase in the f_1 and f_3 factors and finally f_1 becomes very close to f_2. This result is different from that observed for monomer solutions, and we tentatively propose it to be a signature of oligomerisation.

For HC the ratio f_1/f_2 (Fig. 6c) increases by 100% during the first 15 h. The initial quick change slows down gradually in the later stages. Such kinetics may reflect high "consumption" of monomers forming small oligomeric species at the beginning of aggregation. As oligomers get bigger and diffuse slower and monomers become sparser the initial rate of aggregation slows down. The rate of the process can be arbitrary characterised by fitting the f_1/f_2 *vs.* T dependence to the exponential function

$$(f_1/f_2)(T) = (A_0 - A_\infty)\exp[-T/T_{\mathrm{Aggr.}}] + A_\infty \tag{10}$$

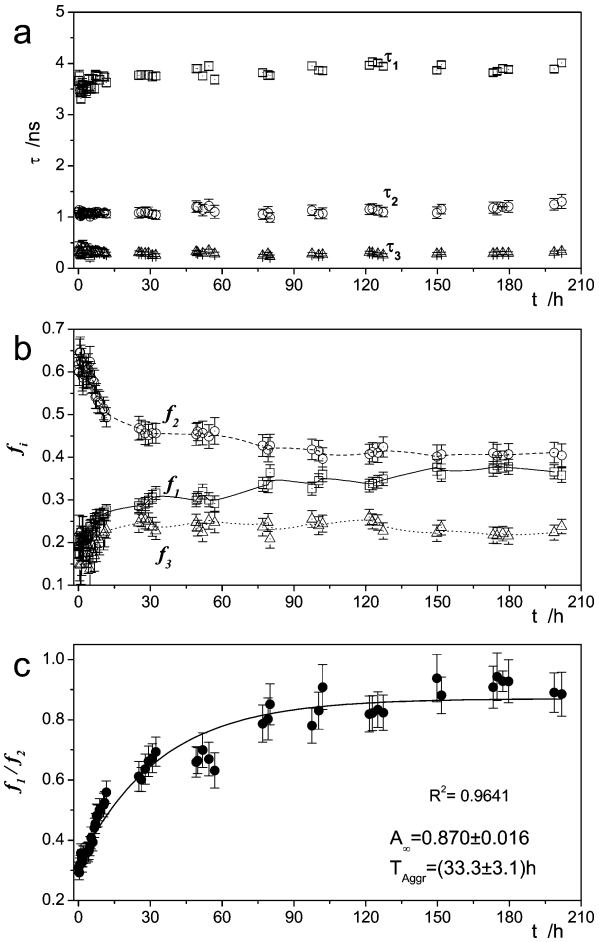

Fig. 6 Parameters obtained from fitting Tyr decay in the HC sample to a 3 exponential decay model. (a) Tyr fluorescence decay time; (b) fluorescence intensity fractional contributions. (c) ratio between decay times fractional contributions f_1/f_2; data according to eqn (10).

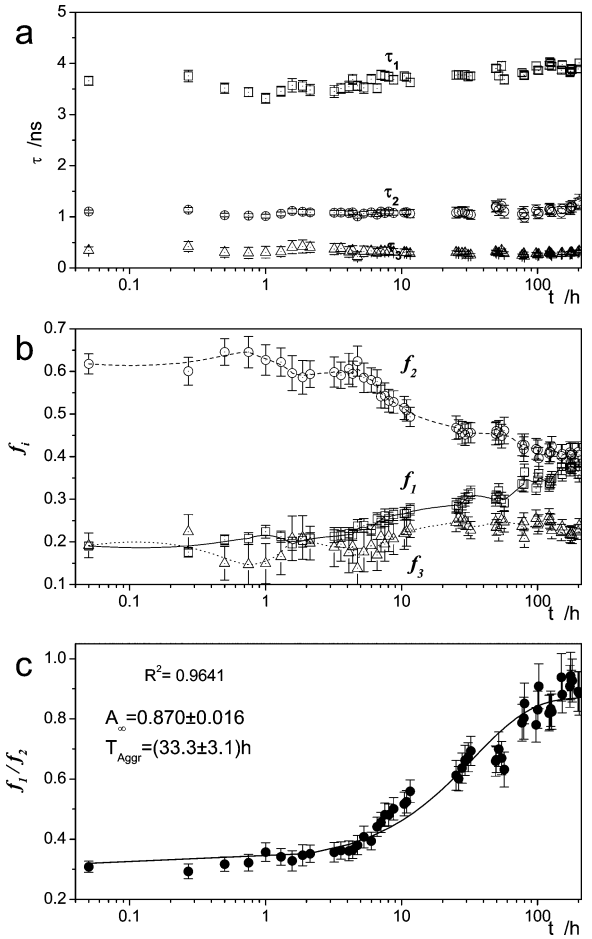

Fig. 7 Data of Fig. 6 shown on a logarithmic time scale.

with A_0 and A_∞ being technical parameters and $T_{\mathrm{Aggr.}}$ a characteristic "aggregation time", which in our experiment achieved a value of 33.3 ± 3.1 h.

The results in Fig. 6 are shown on a logarithmic time scale in Fig. 7 to reveal additional features of the initial hours of aggregation. A slow increase in f_1 and decrease in f_2 (Fig. 7b) are observed during the first 3 h, followed by much more rapid change in f_1 and f_2 at later times. This is reflected in the f_1/f_2 *vs.* time plot (Fig. 7c), where a substantial increase in the f_1/f_2 gradient is observed at the time of about 3 h. Possibly this dramatic change indicates the change in the dominating mechanism of aggregation: from binding of single Aβ peptides to form small structures (dimmers, trimers, *etc.*) that occur in a small proportion of collisional encounters, to aggregation of these structures to form oligomers containing mis-folded sub-structures to which monomers are more likely to adhere when colliding.

Fluorescence decays of the HC sample were also measured at the different emission wavelengths $I(t;T > 210\ \mathrm{h},\lambda)$. As the HC sample showed no further decay evolution for $T > 210$ h, it was regarded as a stable sample where Aβ has aggregated into the final fibrillar structure (see S.E.M. image on Fig. 8d). The fluorescence decays were again fitted to a 3 exponential decay model and the retrieved parameters are shown in Fig. 8a and b. Fig. 8a shows that the lifetimes increase substantially with an increase in the detected wavelength. This suggests that, same as in the monomer, the orientational relaxation of the phenol groups in the aggregated sample are slow and comparable to the fluorescence lifetimes.

Again, the relative changes in these three lifetimes, *i.e.* $(\tau_i(324\ \mathrm{nm}) - \tau_i(300\ \mathrm{nm}))/\tau_i(300\ \mathrm{nm})$ are quite different for each rotamer, namely 0.64, 1.10 and 3.16 ns for Y_1, Y_2 and Y_3, respectively.

A comparison of the lifetime changes in two presented samples (Fig. 5a and 8a) reveals that the effect is present in both, but is more pronounced in the aggregated sample. This allows us to conclude, that, assuming a 3-exponential model of the kinetics, the aggregation additionally slows down the relaxation of rotamers, which is consistent with the local environment of the rotamers being gradually more viscous with aggregation progressing.

The retrieved data were used to create DAS shown in Fig. 8c. In the aggregated peptide the rotamer with the smallest lifetime, Y_3, is quenched as compared to the other two forms and appears to be red shifted in comparison with the non-aggregated sample. Also Y_2, the medium lifetime rotamer, shows a slight red-shifted emission (≈1 nm). Using eqn (9) for the HC data allows estimation of concentrations of individual rotamers. Taking the total HC sample concentration

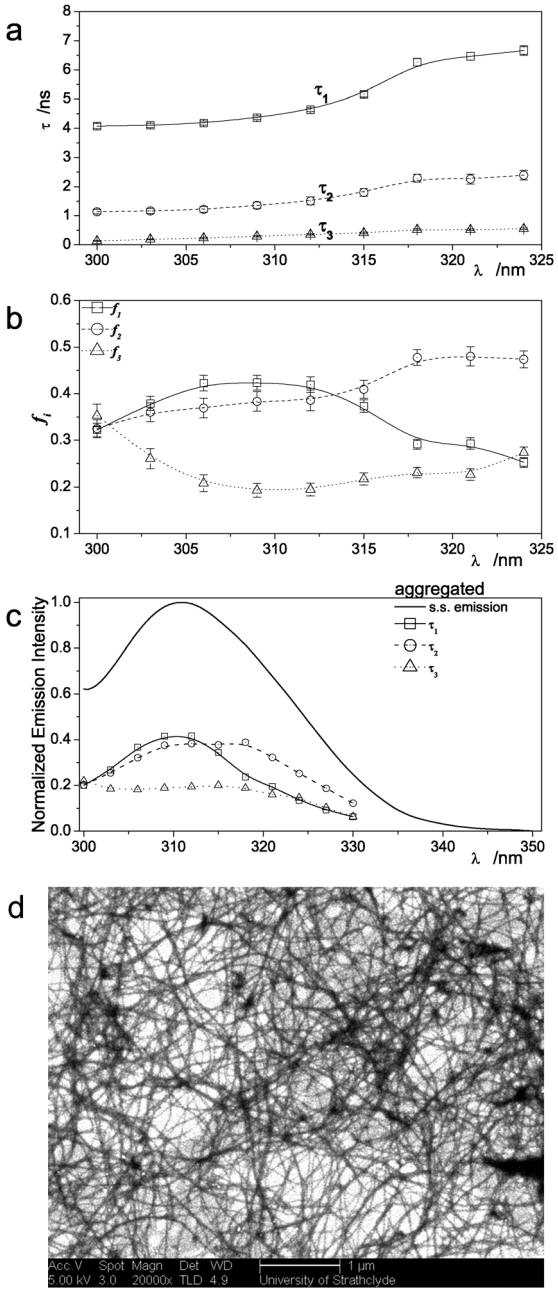

Fig. 8 Parameters obtained from fitting Tyr decay in the HC sample. (a) fluorescence decay times obtained from fitting Tyr decay to a 3 exponential decay model as function of wavelength; (b) fluorescence intensity fractional contributions; (c) full line: emission spectra of Aβ's Tyr; dotted lines: Decay Associated Spectra for the three retrieved decay times; All experimental errors are 3 standard deviations. (d) SEM image of sample HC (taken before lifetime measurements at different wavelengths were performed) confirming the existence of mature amyloid fibrils.

of 50 μM, we obtained 3.62 μM (7.25%), 15.98 μM (31.96%), and 33.39 μM (60.79%) for Y_1, Y_2 and Y_3, respectively. Comparing these percentage contributions with the percentages obtained for the LC sample, shows that the peptide aggregation is an additional factor, together with the bulk peptide concentration, which affects the selection of a rotameric form by individual tyrosines.

Table 1 Peak positions of fluorescence spectra, fluorescence lifetimes and relative concentrations of the rotamers of Tyr in monomer solution and fully aggregated Aβ peptides

	Rotamer	λ_{max}/nm	τ/ns (at 300 nm)	$[Y_i]$/%
[Aβ] monomers	Y_1	311	3.9	4.45
	Y_2	312	0.8	15.10
	Y_3	310	0.1	80.45
[Aβ] aggregates	Y_1	310	4.1	7.25
	Y_2	313	1.1	31.96
	Y_3	314	0.1	60.79

Conclusions

This research has confirmed and extends our previous finding,[14] in that the intrinsic fluorescence of Tyr in Aβ peptide can be useful for monitoring of very early stages of single Aβ peptide-to-peptide aggregation. This result is of fundamental importance in the research on the mechanisms of neurodegenerative diseases, because no other experimental technique enables detection of binding of single peptides noninvasively. Using this approach we have demonstrated, that the initial peptide concentration influences what rotameric conformations are taken by individual peptides (Fig. 3c), and determines the rate of their aggregation (Fig. 4c and 6c). At low Aβ concentrations ($\leq$5 μM), the aggregation is negligible, while at higher concentrations ($\approx$50 μM), the rate of aggregation can be described by exponential change of the f_1/f_2 ratio as a function of time, with the aggregation time of $\approx$33 h.

A three-rotamer model can be effectively used to interpret main fluorescence properties of both the monomer solution and the fully aggregated Aβ peptides. The parameters of rotamers, estimated from the steady-state and lifetime data are collected in Table 1. Comparing the numbers characterising monomers and aggregated forms shows, that the parameters most sensitive to aggregation are relative concentrations of individual rotamers. Therefore fitting the Aβ lifetime data to a 3-exponential model and estimating the relative concentrations of rotamers can be helpful in assessing the state of aggregation. On the other hand, the gradual increase in lifetimes with emission wavelength observed for the both monomer and aggregated samples indicates, the actual Aβ excited-state kinetics is complex and a more advanced modelling of Tyr photophysics is needed to reveal a full information on Aβ aggregation offered by intrinsic fluorescence.

Acknowledgements

The authors thank EPSRC and SFC for financial support including a Science and Innovation Award and Dr P. Edwards for his help with obtaining the SEM image.

References

1 M. Stefani and C. M. Dobson, *J. Mol. Med.*, 2003, **81**, 678–699.
2 D. M. Walsh and D. J. Selkoe, *J. Neurochem.*, 2007, **101**, 1172–1184.
3 K. N. Dahlgren, A. M. Manelli, W. B. Stine, L. K. Baker, G. A. Krafft and M. J. LaDu, *J. Biol. Chem.*, 2002, **277**, 32046–32053.
4 M. P. Marzolo and G. J. Bu, *Semin. Cell Dev. Biol.*, 2009, **20**, 191–200.

5 N. Carullaa, M. Zhou, M. Arimon, M. Gairi, E. Giralt, C. V. Robinson and C. M. Dobson, *Proc. Natl. Acad. Sci. U. S. A.*, 2009, **106**, 7828–7833.
6 T. R. Serio, A. G. Cashikar, A. S. Kowal, G. J. Sawicki, J. J. Moslehi, L. Serpell, M. F. Arnsdorf and S. L. Lindquist, *Science*, 2000, **289**, 1317–1321.
7 N. Benseny-Cases, M. Cocera and J. Cladera, *Biochem. Biophys. Res. Commun.*, 2007, **361**, 916–921.
8 V. I. Stsiapura, A. A. Maskevich, V. A. Kuzmitsky, V. N. Uversky, I. M. Kuznetsova and K. K. Turoverov, *J. Phys. Chem. B*, 2008, **112**, 15893–15902.
9 L. A. Munishkina and A. L. Fink, *Biochim. Biophys. Acta, Biomembr.*, 2007, **1768**, 1862–1885.
10 M. R. H. Krebs, E. H. C. Bromley and A. M. Donald, *J. Struct. Biol.*, 2005, **149**, 30–37.
11 S. Thirunavukkuarasu, E. A. Jares-Erijman and T. M. Jovin, *J. Mol. Biol.*, 2008, **378**, 1064–1073.
12 J. Kaylor, N. Bodner, S. Edridge, G. Yamin, D. P. Hong and A. L. Fink, *J. Mol. Biol.*, 2005, **353**, 357–372.
13 S. A. Kim and P. Schwille, *Curr. Opin. Neurobiol.*, 2003, **13**, 583–590.
14 O. Rolinski, M. Amaro and D. Birch, *Biosens. Bioelectron.*, 2010, **25**, 2249–2252.
15 C. Lee, A. Nayak, A. Sethuraman, G. Belfort and G. Mcrae, *Biophys. J.*, 2007, **92**, 3448–3458.
16 J. R. Unruh, M. R. Liyanage and C. K. Johnson, *J. Phys. Chem. B*, 2007, **111**, 5494–5502.
17 W. B. Stine, K. N. Dahlgren, G. A. Krafft and M. J. LaDu, *J. Biol. Chem.*, 2003, **278**, 11612–11622.
18 C. D. McGuinness, K. Sagoo, D. McLoskey and D. J. S. Birch, *Meas. Sci. Technol.*, 2004, **15**, L19–L22.